Molecular Orbital Studies of the Intramolecular Reaction of Protonated *cis*- and *trans*-3,4-Epoxypentan-1-ol

James M. Coxon,*,† Keiji Morokuma,‡ Aaron J. Thorpe,† and Dale Whalen§

Department of Chemistry, University of Canterbury, Christchurch, New Zealand, University of Maryland, Baltimore County Campus, Baltimore, Maryland, and Cherry L. Emerson Center for Scientific Computation and Department of Chemistry, Emory University, Atlanta, Georgia 30322

Received November 11, 1997

The transition structures for the intramolecular reaction of protonated *cis*- and *trans*-3,4-epoxypentan-1-ol (**13**) and (**16**), which result in the formation of protonated *cis*- and *trans*-2-methylfuran-3-ols (**14**) and (**18**) with inversion and retention, have been determined at the ab initio MP2/6-31G* and hybrid density functional B3LYP/6-31G* levels of theory. Intrinsic reaction coordinate calculations for the lower energy inversion pathways for formation of the 2-methylfuran-3-ols show that intramolecular attack occurs in concert with ring opening. The reaction pathways are far from optimum for best orbital overlap, reflecting the strained bicyclic nature of the transition structures.

Introduction

Empirical rules elaborated by Baldwin[1] for predicting the regiochemistry of ring-closure reactions are used as a guide in planning the synthesis of cyclic molecules. For example, a reaction that forms a strainless or near strainless five- or six-membered ring generally occurs readily; however, ring closure is disfavored when it involves reaction at a trigonal carbon atom that forms a double bond to an atom inside the incipient ring (the 5-*endo-trig* system). In contrast, 5-*exo-trig* reactions are successful when reaction is at a double bond that is *outside* the incipient ring (Figure 1).

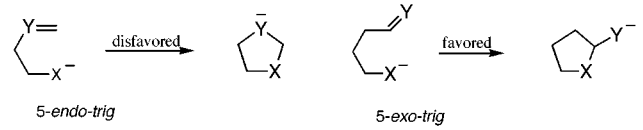

Figure 1. 5-*Endo* and *exo-trig* cyclization.

Ring opening of epoxides with a proton or Lewis acid is an important method of initiating intramolecular ring closure. For example *trans*-5,6-epoxyheptan-1-ol (**1b**) ($n = 4$) reacts with BF_3 to give (1*SR*,2′*RS*)-1-(tetrahydropyran-2′-yl)ethanol (**2**) (>95%) in preference to formation of *trans*-2-methyloxepan-3-ol (**3**) (3%) (Figure 2).[2] Both products are the result of reaction occurring with inversion of configuration at the site of nucleophilic attack. For *trans*-4,5-epoxyhexan-1-ol (**1a**) ($n = 3$), five-membered ring formation to give (1*SR*,2′*RS*)-1-(tetrahydrofuran-2′-yl)ethanol (**4**) competes with formation of *trans*-2-methyltetrahydropyran-3-ol (**5**) (4:1) (Figure 2) with both products a result of inversion of configuration at the site of nucleophilic attack.

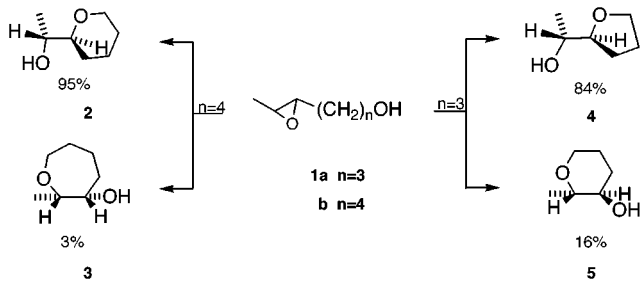

Figure 2. Acid-catalyzed rearrangement of *trans*-5,6-epoxyheptan-1-ol and *trans*-4,5-epoxyhexan-1-ol.

Recently, Janda and Lerner[3] developed a catalytic antibody to overcome the stereoelectronic preference for five- over six-membered ring formation and catalyze the rearrangement of *trans*-7-aryl-4,5-epoxyheptan-1-ol **6** to the 6-*endo-tet* product **8** rather than give the tetrahydropyran **7**, the major product in the absence of the catalytic antibody (see Figure 3).[4]

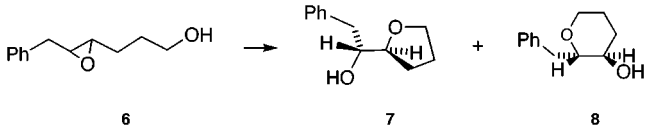

Figure 3. Intramolecular rearrangement of *trans*-7-aryl-4,5-epoxyheptan-1-ol **6** to 6-*endo-tet* product **8** and tetrahydropyran **7**.

Houk has carried out calculations at the MP2 level for a model system *trans*-5,6-epoxyheptan-1-ol (**1a**) lacking the aryl group (Figure 2). Specifically, the barrier that needs to be overcome by the catalytic antibody was calculated. The 5-*exo* process is calculated to be favored by 1.9 kcal/mol. Assuming a negligible entropic difference in the two transition structures, this translates to a 96:4 product ratio at 25 °C:[4] "To favor the 6-*endo* product **5** to a similar amount, the catalytic antibody must lower the 6-*endo* activation energy 3.6 kcal/mol

* To whom correspondence should be addressed. E-mail: J.Coxon@csc.canterbury.ac.nz.
† University of Canterbury.
‡ Emory University.
§ University of Maryland.

(1) Baldwin, J. E. *J. Chem. Soc., Chem. Commun.* **1976**, 734. See also: Norman, Sir R.; Coxon, J. M. *Principles of Organic Synthesis* Blackie Chapman and Hall: London, and John Wiley and Sons: New York, 1993; p 678.
(2) Coxon, J. M.; Hartshorn, M. P.; Swallow, W. H. *Aust. J. Chem.* **1973**, *26*, 2521.
(3) Janda, K. D.; Shevlin, C. G.; Lerner, R. A. *Science* **1993**, *259*, 490.

S0022-3263(97)02071-9 CCC: $15.00
Published on Web 05/22/1998

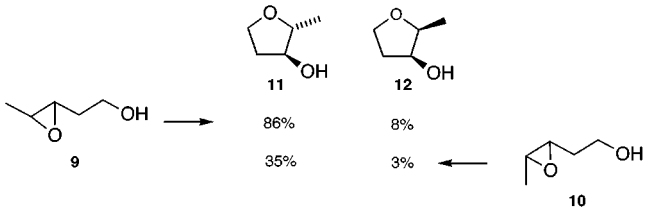

Figure 4. Acid-catalyzed rearrangement of **9** and **10**.

more than it lowers the 5-*exo* activation barrier." Furthermore, some imaginative calculations have been used to show the effect of a proximate acid source and counterion in influencing transition-state structure, thereby mimicking the regiochemistry dictated by the catalytic antibody.[5]

The boron trifluoride-catalyzed reaction of *trans*- and *cis*-3,4-epoxypentan-1-ol (**9** and **10**) in diethyl ether results in the formation of *trans*- and *cis*-2-methylfuran-3-ols (**11**) and (**12**) (Figure 4). There is no evidence in either reaction for the formation of the more strained four-membered ring ether. The trans-isomer **9** gives predominantly, and in high yield, *trans*-2-methylfuran-3-ol (**11**), the product resulting from inversion of configuration at the reaction center. The mechanism for formation of the lesser cis-isomer **12** is in doubt. It could be formed via an intermediate fluorohydrin or by nucleophilic attack with retention of configuration. The *cis*-epoxide **10** is unusual in that it gives a predominance of the same *trans*-2-methylfuran-3-ol (**11**), a product, in this case at least formally, of retention of configuration at the reaction center.[2] It is again not known if the predominance of this product is the result of a mechanism involving retention of configuration at the site of nucleophilic attack or if the reaction involves a fluorohydrin and two sequential inversion reactions.

We have sought to investigate the reaction of the protonated form of **9** and **10** using ab initio and density functional methods to determine stationary points in an effort to quantify electronic and steric factors and further examine the pathway for ring formation via intrinsic reaction coordinate calculations.[6]

Computational Methods

Exploratory calculations were carried out at semiempirical AM1[7] and Hartree−Fock 3-21G* and 6-31G* levels. The results reported here, including optimized structures, vibrational frequencies, and intrinsic reaction coordinate (IRC) calculations, were obtained at the ab initio MP2/6-31G*(Full) and the gradient-corrected hybrid density functional B3LYP/6-31G*[8] levels of theory. We have examined the stationary points at both levels of theory to validate the appropriateness of the less expensive B3LYP method.[9] All stationary points were identified for the number of imaginary frequencies by vibrational frequency analysis. Zero-point corrections (ZPC) are included in any relative energies with B3LYP/6-31G* and MP2/6-31G* zero-point vibrational energies scaled by 0.961 and 0.95, respectively. The GAUSSIAN 94[10] suite of programs was used throughout the present work.

Results and Discussion

We now report results of ab initio and density functional calculations of the transition structures for the intramolecular rearrangement of the protonated form of *trans*- and *cis*-3,4-epoxypentan-1-ol (**9**) and (**10**) involving *inversion* of configuration at the site of intramolecular nucleophilic attack that result in formation of the protonated form of *trans*- and *cis*-2-methylfuran-3-ols (**11**) and (**12**) and the corresponding 1-(oxacyclobutan-2′-yl)ethanols. We also report transition structures for formation of **11** and **12** with *retention* of configuration.

Acid-catalyzed rearrangement and addition to epoxides is considered to occur via the intermediacy of the protonated or Lewis acid-coordinated epoxide oxygen.[11] Protonation can occur from either face of the epoxide ring to give the stereoisomeric syn and anti oxonium ions.[11] Calculations carried out on the proton-catalyzed rearrangement of propene oxide[12] show the syn-protonated oxonium ion is marginally higher in energy than the anti diastereomer. Therefore, if hydrogen bonding effects are neglected, protonation of *cis*-3,4-epoxypentan-1-ol (**10**) would be expected to be favored on the less hindered face of the epoxide (i.e., **13**, Figure 5), while for the *trans*-3,4-epoxypentan-1-ol (**9**), the faces are hindered more equally.

Potential Energy Surface for Rearrangement of Protonated *cis*-3,4-Epoxypentan-1-ol (13). Conformations of Protonated *cis*-3,4-Epoxypentan-1-ol (13), Protonated *cis*-2-Methylfuran-3-ol (14), and Protonated 1-(Oxacyclobutan-2′-yl)ethanol (15). The lowest energy conformation of the reactant, *anti*-protonated *cis*-3,4-epoxypentan-1-ol (**13**),[13] is shown in Figure 5. The corresponding syn diastereomer **17**[13] is lower in energy (ca. 11 kcal/mol both at the MP2/6-31G* and the B3LYP/6-31G* level) (Figure 6),[14] a result of hydrogen bonding between $OH10^+$ of the protonated epoxy group and the alcohol oxygen. Protonated *cis*-2-methylfuran-3-ol (**14**)[13,15] and protonated 1-(oxacyclobutan-2′-yl)ethanol **15**[13] are the two possible products of intramolecular rearrangement of **13** with inversion (Figure 5).

Transition States for Rearrangement of Protonated *cis*-3,4-Epoxypentan-1-ol (13) and (17). We first report the rearrangement of anti-protonated *cis*-3,4-epoxypentan-1-ol (**13**). This protonated structure was originally obtained at the completion of an IRC calculation at the MP2/6-31G* level from **TS 13−14** and shown to in fact be a global minima. The two transition

(4) Na, Houk, J.; Shevlin, K. N.; C. G.; Janda, Lerner, K. D.; R. A. *J. Am. Chem. Soc.* **1993**, *115*, 8453.
(5) Na, J.; Houk, K. N. *J. Am. Chem. Soc.* **1996**, *118*, 9204.
(6) Methods defined herein: Coxon, J. M.; Houk, K. N.; Luibrand, R. T. *J. Org. Chem.* **1995**, *60*, 418−427.
(7) AM1: Dewar, M. J. S.; Zoebisch, E. G.; Healy, E. F.; Stewart, J. J. P. *J. Am. Chem. Soc.* **1985**, *107*, 3902.
(8) (a) Becke, A. D. *Phys. Rev. A* **1988**, *38*, 3098. (b) Becke, A. D. *J. Chem. Phys.* **1993**, *98*, 1372. (c) Lee, C.; Yang, W.; Parr, R. G. *Phys. Rev. B* **1988**, *37*, 785.
(9) Cf. Schreiner, P. R.; Schleyer, P. v. R.; Schaefer, H. F. *J. Org. Chem.* **1997**, *62*, 4216.
(10) Gaussian 94, Revision B.1. Frisch, M. J.; Trucks, G. W.; Schlegel, H. B.; Gill, P. M. W.; Johnson, B. G.; Robb, M. A.; Cheeseman, J. R.; Keith, T.; Petersson, G. A.; Montgomery, J. A.; Raghavachari, K.; Al-Laham, M. A.; Zakrzewski, V. G.; Ortiz, J. V.; Foresman, J. B.; Cioslowski, J.; Stefanov, B. B.; Nanayakkara, A.; Challacombe, M.; Peng, C. Y.; Ayala, P. Y.; Chen, W.; Wong, M. W.; Andres, J. L.; Replogle, E. S.;. Gomperts, R.; Martin, R. L.; Fox, D. J.; Binkley, J. S.; Defrees, D. J.; Baker, J.; Stewart, J.; P.; Head-Gordon, M.; Gonzalez, C.; Pople, J. A. Gaussian, Inc., Pittsburgh, PA, 1995.
(11) Ford, G. P.; Smith, C. T. *J. Am. Chem. Soc.* **1987**, *109*, 1325.
(12) Coxon, J. M.; Maclagan, R. G. A. R.; Rauk, A.; Thorpe, A. J.; Whalen, D. *J. Am. Chem. Soc.* **1997**, *119*, 4712−4718.
(13) See the Supporting Information for the method of generation of the structure.
(14) The direct rearrangement between the diastereomers **13** and **17** is unlikely, as suggested by a high transition state energy (ca. 17 kcal/mol at MP2/6-31G*) between the invertomers of protonated propene oxide.[12] Therefore, these two protonated diastereomers are likely to be in equilibrium via reversible protonation/deprotonation, and **17** is the most abundant protonated form of the *cis*-epoxide.

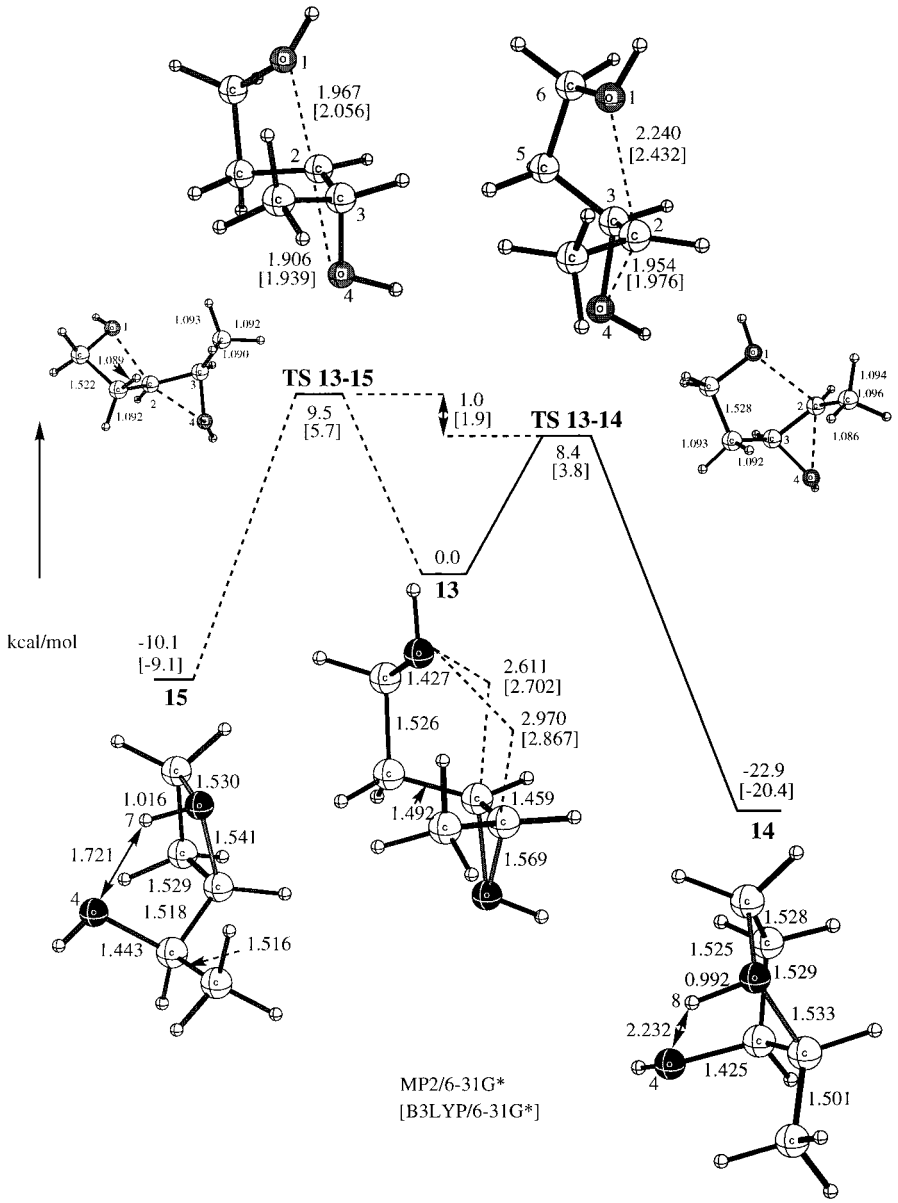

Figure 5. Potential energy profile for rearrangement of protonated *cis*-3,4-epoxypentan-1-ol (**13**) to **14** and **15**, both with retention of configuration. Geometries (in Å and deg) at the MP2(full)/6-31G* level. Two perspectives of each transition structure are shown. The relative energies in two levels (MP2(full)/6-31G*, B3LYP/6-31G* in brackets) are in kcal/mol and include zero-point corrections.

structures for rearrangement with inversion of **13** to protonated 1-(oxacyclobutan-2′-yl)ethanol (**15**) and protonated *cis*-2-methylfuran-3-ol (**14**) are shown in Figure 5 with the corresponding energies with zero-point corrections given in Tables 1 and 2.

The five-membered transition structure **TS 13**−**14**[16] is favored over the four-membered transition structure **TS 13**−**15** at all levels of theory studied. A notable difference between the four- and five-membered transition structures for inversion is that in the former the forming and the breaking C−O bonds are of comparable length (difference of 0.06 Å at the MP2/6-31G* level) while in the latter the difference between the two is much larger (0.29 Å). The C−O distances in **TS 13**−**14** are substantially longer than the corresponding distances in **TS 13**−**15**. One may say that **TS 13**−**14** is an *earlier* and substantially *looser* transition state than **TS 13**−**15**. The larger exothermicity of the reaction **13** → **14** compared to **13** → **15** is consistent with the earlier transition state for the former. The looseness of **TS 13**−**14** must be related to the distance that the oxygen atom of the hydroxyl has to travel from the reactant **13** (a HO···C distance of 2.97 Å at the MP2/6-31G* level, see Figure 5) to the reaction **TS 13**−**14** (2.24 Å), as compared with the corresponding distance from **13** (2.61 Å) to **TS 13**−**15** (1.97 Å). The path of reaction for **TS 13**−**14** is longer than that for **TS 13**−**15**, and the forming O−C bond is still weak at **TS 13**−**14**. A selection of CC and CH bond distances are given in Figure 5. There is no evidence for significant hyperconjugation from CH's of the methyl adjacent to the reaction center for the five-

(15) The lowest energy conformer **14** with the ether proton syn to the hydroxyl was 5.4 kcal/mol lower in energy than the lowest energy structure protonated anti to the hydroxyl and has a hydrogen bond between O4 and H8 (2.232 Å at MP2/6-31G*). The O1−H8 bond (0.992 Å) is somewhat longer than it would be in the absence of this H-bonding.

(16) **TS 13**−**14** was calculated to be lower in energy by 1.0 kcal/mol (HF/6-31G* + ZPC) than when the proton was positioned syn to the epoxide substituent groups; therefore, the IRC was conducted from the anti-protonated structure (**TS 13**−**14**) even though **17** (Figure 6) is lower than **13**.

Table 1. Energies of Transition States (ZPC Scaled by 0.95 (MP2), 0.961 (B3LYP), and 0.8929 (HF))

transition structures		energy (au)	ZPVE (au)	energy + scaled ZPC(au)	diff 4m−5m TS (kcal/mol)	imag freq
TS 13−14	optimized					
	HF	−345.161 48	0.170 11	−345.009 59	3.53	249
	MP2 (full)	−346.181 67	0.162 06	−346.027 71	1.04	438
	B3LYP/6-31G*	−347.271 63	0.158 69	−347.119 13	1.94	300
	single point at MP2 geom					
	HF	−345.155 14	0.162 06	−345.001 18	4.74	
	MP2 (fc)	−346.152 08	0.162 06	−345.998 12	1.01	
	MP3	−346.197 87	0.162 06	−346.043 91	2.23	
	MP4D	−346.221 35	0.162 06	−346.067 40	1.91	
	MP4DQ	−346.205 49	0.162 06	−346.051 53	2.12	
	MP4SDQ	−346.217 33	0.162 06	−346.063 37	1.71	
	MP4SDTQ	−346.248 80	0.162 06	−346.094 84	0.99	
TS 13−15	optimized					
	HF	−345.156 20	0.170 49	−345.003 97		252
	MP2 (full)	−346.180 64	0.162 73	−346.026 05		483
	B3LYP/6-31G*	−347.269 30	0.159 48	−347.116 04		310
	single point at MP2 geom					
	HF	−345.148 23	0.162 73	−344.993 64		
	MP2 (fc)	−346.151 12	0.162 73	−345.996 52		
	MP3	−346.194 96	0.162 73	−346.040 36		
	MP4D	−346.218 95	0.162 73	−346.064 36		
	MP4DQ	−346.202 75	0.162 73	−346.048 16		
	MP4SDQ	−346.215 25	0.162 73	−346.060 65		
	MP4SDTQ	−346.247 86	0.162 73	−346.093 27		
TS 16−18	optimized					
	HF	−345.166 05	0.170 28	−345.014 01	5.19	208
	MP2 (full)	−346.186 99	0.162 00	−346.033 09	3.54	393
	B3LYP/6-31G*	−347.276 94	0.158 84	−347.124 29	3.97	233
	single point at MP2 geom					
	HF	−345.160 15	0.162 00	−345.006 25	6.76	
	MP2 (fc)	−346.157 37	0.162 00	−346.003 48	3.48	
	MP3	−346.203 00	0.162 00	−346.049 11	4.52	
	MP4D	−346.226 46	0.162 00	−346.072 57	4.21	
	MP4DQ	−346.210 55	0.162 00	−346.056 66	4.42	
	MP4SDQ	−346.222 36	0.162 00	−346.068 47	3.99	
	MP4SDTQ	−346.253 82	0.162 00	−346.099 93	3.28	
TS 16−21	optimized					
	HF	−345.157 86	0.170 38	−345.005 74		258
	MP2 (full)	−346.181 90	0.162 58	−346.027 45		485
	B3LYP/6-31G*	−347.271 12	0.159 37	−347.117 97		312
	single point at MP2 geom					
	HF	−345.149 93	0.162 58	−344.995 48		
	MP2 (fc)	−346.152 38	0.162 58	−345.997 93		
	MP3	−346.196 35	0.162 58	−346.041 90		
	MP4D	−346.220 31	0.162 58	−346.065 86		
	MP4DQ	−346.204 07	0.162 58	−346.049 62		
	MP4SDQ	−346.216 56	0.162 58	−346.062 11		
	MP4SDTQ	−346.249 15	0.162 58	−346.094 70		
TS 17−18	optimized					
	HF	−345.150 95	0.169 99	−344.999 17		174
	MP2 (full)	−346.166 88	0.161 08	−346.013 85		248
	B3LYP/6-31G*	−347.261 76	0.157 92	−347.110 00		209
TS 22−14	optimized					
	HF	−345.154 16	0.169 45	−345.002 86		223
	MP2 (full)	−346.168 43	0.160 92	−346.015 56		308
	B3LYP/6-31G*	−347.262 95	0.1578	−347.111 30		257

membered transition structure or from analogous CH and CC bonds for the four-membered transition structure.

To be able to use calculations to predict the reaction regiochemistry, in this case the preference for five- over four-membered ring formation, the correct description of the energy difference between **TS 13−15** and **TS 13−14** is essential. This difference changes from 1.0 kcal/mol at MP2/6-31G*, 2.2 kcal/mol at MP3 (frozen core), 1.7 kcal/mol at MP4SDQ (frozen core) to 1.0 kcal/mol at MP4SDTQ (frozen core). Although one has to also examine the effects of larger basis sets in order to obtain fully converged results, there appears to be no doubt that **TS 13−14** is a few kcal/mol lower than **TS 13−15**. There is no experimental evidence for products of a four-membered transition structure. However, the calculated **TS 13−15** is only 1.0 kcal/mol (MP2/6-31G*) and 1.9 (B3LYP) higher than **TS 13−14**, which suggests that the B3LYP result is more consistent with experiment.

The major product of reaction of **10** with boron trifluoride was **11**, a product that cannot be formed by a route involving inversion of configuration. We were able to find a transition structure that retains the configuration. This transition state **TS 17−18** results from reaction of the more stable *syn*-protonated epoxide diastereomer **17**. The energy of this transition structure (Figure 6) is 8.6 (MP2/6-31G*) and 5.7 kcal/mol (B3LYP/6-31G*) higher than

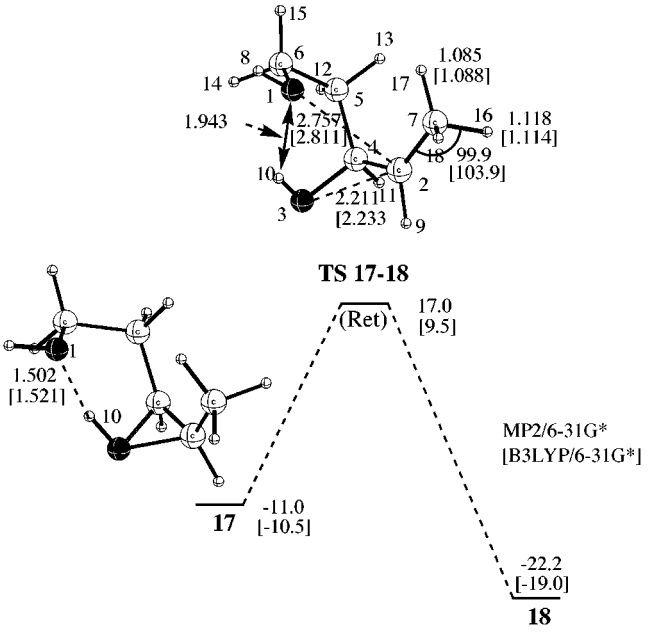

Figure 6. Potential energy profile for rearrangement of **17** to **18** with retention of configuration, compared with that of **13** to **14**. Geometries (in Å and deg) at the MP2(full)/6-31G* level. The energies relative to **13** in two levels (MP2(full)/6-31G*, B3LYP/6-31G* in brackets) are in kcal/mol and include zero point corrections.

Table 2. Energies of Minima (ZPC Scaled by 0.95 (MP2), 0.961 (B3LYP), and 0.8929 (HF))

minima		energy (au)	ZPVE (au)	energy + scaled ZPC (au)
13	optimized			
	HF	−345.167 72	0.172 25	−345.013 92
	MP2 (full)	−346.196 31	0.163 57	−346.040 92
	B3LYP/6-31G*	−347.279 09	0.160 12	−347.125 21
14	optimized			
	HF	−345.205 57	0.174 42	−345.049 83
	MP2 (full)	−346.235 15	0.165 97	−346.077 48
	B3LYP/6-31G*	−347.313 66	0.162 29	−347.157 70
15	optimized			
	HF	−345.182 99	0.173 99	−345.027 63
	MP2 (full)	−346.213 87	0.165 07	−346.057 05
	B3LYP/6-31G*	−347.295 31	0.161 96	−347.139 67
16	optimized			
	HF	−345.170 16	0.170 27	−345.018 13
	MP2 (full)	−346.198 55	0.163 43	−346.043 29
	B3LYP/6-31G*	−347.281 52	0.160 08	−347.127 68
17	optimized			
	HF	−345.177 64	0.173 46	−345.022 76
	MP2 (full)	−346.214 33	0.164 03	−346.058 50
	B3LYP/6-31G*	−347.296 65	0.161 05	−347.141 88
18	optimized			
	HF	−345.204 38	0.174 34	−345.048 71
	MP2 (full)	−346.234 19	0.166 14	−346.076 36
	B3LYP/6-31G*	−347.312 01	0.162 81	−347.155 55
21	optimized			
	HF	−345.183 44	0.174 07	−345.028 01
	MP2 (full)	−346.214 41	0.165 20	−346.057 47
	B3LYP/6-31G*	−347.295 68	0.162 10	−347.139 90
22	optimized			
	HF	−345.182 24	0.173 06	−345.027 71
	MP2 (full)	−346.217 34	0.163 69	−346.061 83
	B3LYP/6-31G*	−347.299 70	0.160 55	−347.145 41

TS 13−14, resulting from inversion of configuration from the *anti*-protonated epoxide diastereomer **13**.[17]

The calculated substantially higher energy of the transition state **TS 17−18** compared to **TS 13−14** and the expected equilibrium between **13** and **17** suggests

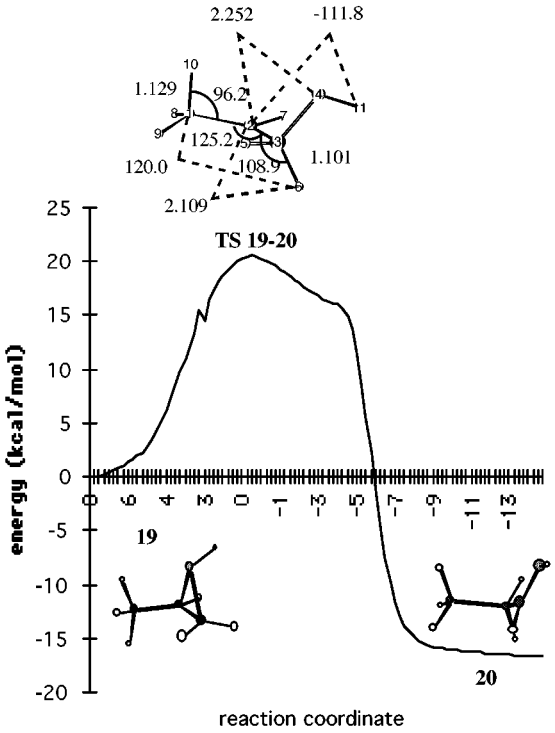

Figure 7. Potential energy profile for rearrangement of protonated propene oxide (**19**) to protonated propanal (**20**) at the MP/2.6-31G* level.

that the reaction with retention via **TS 17−18** to form **11** directly is not likely to occur. In the reaction with $BF_3{\cdot}Et_2O$, the isolation of **11** from **10**, a product of apparent retention of configuration at the site of nucleophilic attack, therefore most probably involves the intermediacy of fluorohydrin.

The transition structure for retention **TS 17−18** shows hyperconjugation between one of the methyl hydrogens and the carbocation center exhibiting a reduced C2−C7−H16 angle of 100° and lengthening of one methyl C−H to 1.118 Å. A comparison with corresponding bonds for the transition structure (**TS 19−20**, Figure 7) for the rearrangement of protonated propene oxide (**19**) to protonated propanal (**20**) show that in the latter a suitably disposed CH adjacent to the developing site of electron deficiency increases to a maxima at the transition geometry of 1.13 Å.[12] This bond length extension, indicative of hyperconjugative stabilization, is not observed for either the intramolecular four- or five-membered transition structures (Figure 5) for inversion of configuration, which is consistent with intramolecular hydroxyl attack being earlier in the reaction coordinate than hydride migrationin the propene oxide rearrangement. Furthermore, the rearrangement of propene oxide exhibits a reaction profile that could be described as asynchronous with two distinct and independent processes that are not linked by the formation of a discrete intermediate (Figure 7).

The first process is rupture of the protonated epoxide, and the second closely following process is hydride migration. These two sequential process are preceded by an initial rotation of the methyl to bring an adjacent CH of the methyl into alignment with the electron-deficient center that subsequently develops.[12] Rotation of the methyl group is not observed in the inversion transition structure for intramolecular ether formation

for protonated *cis*-3,4-epoxypentan-1-ol **13** since the hydroxyl attack at carbon occurs early in the reaction and in concert with epoxide CO bond rupture. Carbonyl formation by hydride migration does not compete with furan formation, consistent with the higher calculated activation barrier for hydride migration.

The barrier to reaction for rearrangement of **13** to **14** (MP2/6-31G* ca. 8.4 kcal/mol) is substantially lower (Figure 5) than for the lowest pathway found for rearrangement of protonated propene oxide to protonated propanal (17.7 MP2/6-31G* kcal/mol).[12] For the intramolecular nucleophilic attack of hydroxyl, the decrease in activation barrier compared with rearrangement of protonated propene oxide is a reflection of the facility of the hydroxyl to participate in concert with cleavage of the protonated epoxide. In contrast, the migrating hydrogen in the rearrangement of protonated propene oxide occurs after epoxide cleavage with consequent charge development at carbon and hyperconjugative stabilization at the transition structure. This results in an asynchronous reaction pathway. In comparison with the reaction of propene oxide, the developing charge at the reaction carbon center of **13** for both the four- and five-membered transition structures is offset by the close proximity of the nucleophile and does not require stabilization by hyperconjugation.

The Intrinsic Reaction Coordinate (IRC) Analysis of the Rearrangement: 13 → TS 13−14 → 14. The intrinsic reaction coordinate (IRC) is the minimum energy path or the path of steepest decent from the transition state to both reactant and product directions with appropriate mass factor taken into account and provides a representative trajectory for the reaction.[18] An IRC calculation was performed at the MP2/6-31G* level for the more favored reaction pathway for **13** involving the five-membered transition structure **TS 13−14**.[19] The energetics (without ZPE) and changes of important geometrical parameters along the IRC (stopped because of computational instability at 3.10 bohr·amu$^{1/2}$ on the reactant side and at −4.07 bohr·amu$^{1/2}$ on the product side) are shown in Figure 8. Analysis of the IRC reveals a number of interesting features of the course of the reaction.

The energy profile for the intramolecular rearrangement of **13** to **14** in Figure 8a reflects a single concerted process.[20] The increase in the C2−O4 bond distance for epoxide opening and the decrease in the O1−C2 distance for the attacking intramolecular nucleophile interaction occur at the same time and nearly linearly (Figure 8b). The O1−C2−C3 angle increases from 67° near structure **13** at the first point of the IRC to 81.7° at the transition structure and 100° approaching **14** at the end of the IRC (Figure 8c). The O1−C2−C3−O4 torsional angle increases from 158.8° and subsequently decreases at the transition structure (160.7°), continuing to decrease to 155.2° near **14** (Figure 8d). The angles at the transition state compare with the bond angle of 104.6° and torsional angle of 177.1° at the HF/6-31G* transition structure for attack of water on ethylene oxide.[11] The preference for the atoms most involved at the reaction center to be in an anti periplanar conformation is compromised by the ring strain of the rupturing protonated epoxide and developing furan ring, and the IRC trajectory is far from optimum overlap of the reacting centers for intramolecular attack. The changes in the O1−C6−C5 and C6−C5−C3 bond angles are representative of internal bond angle variation as the reaction proceeds, reflecting the compromise between optimizing the overlap of the reacting center and the conformational requirements associated with the development of the five-membered ring (Figure 8e).

Overall, the IRC reveals clearly that the relief of the strain in the epoxide ring and the nucleophilic attack of the hydroxyl to the epoxide from the reverse face at the site of epoxide cleavage take place at the same time.

Potential Energy Surface for Rearrangement of Protonated *trans*-3,4-Epoxypentan-1-ol (16). Conformations of Protonated *trans*-3,4-Epoxypentan-1-ol (16), Protonated *trans*-2-Methylfuran-3-ol (18), and Protonated 1-(Oxacyclobutan-2′-yl)ethanol (21). The lowest energy conformations of the reactant, protonated *trans*-3,4-epoxypentan-1-ol, and the two products, protonated *trans*-2-methylfuran-3-ol (**18**) and protonated 1-(oxacyclobutan-2′-yl)ethanol (**21**), are shown in Figure 9.[13] The lowest energy structure, **18**, optimized at the MP2/6-31G* level in Figure 9, shows intramolecular hydrogen bonding (2.155 Å) between the ether proton and the hydroxyl oxygen.

Transition States for Rearrangement of Protonated *trans*-3,4-Epoxypentan-1-ol (16). The transition structures for formation of **18** and **21** from protonated **16** are shown in Figure 9. For the inversion pathways, there is no evidence for hyperconjugation from CH's of the methyl adjacent to the reaction center for the five-membered transition structure or from analogous CH and CC bonds for the four-membered transition structure. The four-membered transition structure **TS 16−21**, analogous to **TS 13−15**, is tighter than the five-membered transition structure **TS 16−18**. For the former, the bond distances from the reaction carbon center to the two oxygens are comparable (1.961 and 1.907 Å), while the corresponding values for the five-membered transition state are larger and more asymmetric, with cleavage of the C−O bond of the epoxide more advanced than intramolecular hydroxyl attack. The **TS 16−18** is marginally tighter than the corresponding **TS 13−14**. It is perhaps surprising that the difference in geometry between the four- and five-membered transition structures is greater for **13** than **16**. For the former, both the four- and five-membered transition structures are congested by the methyl cis to the hydroxymethylene chain. For **16**, the trans nature of the epoxide allows for some relief of this congestion, yet the difference in energy between the four- and five-membered ring transition structures becomes larger, 3.5 kcal/mol for **16** at the MP2/6-31G* level vs 1.0 kcal/mol for **13**.

The calculated barrier (6.6 kcal/mol at MP2/6-31G*) at **TS 16−18** is lower than that for the lowest asynchronous concerted pathway for rearrangement of protonated propene oxide to protonated propanal (17.7 kcal/mol). For the diastereomeric protonated epoxide **16**, the ability of

(17) Another transition structure involving retention of configuration for the conversion of **13** to **18** was found at the HF/3-21G* level with a high barrier of 14.3 kcal/mol (HF/3-21G* + ZPC). However, this structure does not exist at higher levels of theory.

(18) Fukui, K.; Kato, S.; Fujimoto, H. *J. Am. Chem. Soc.* **1975**, *97*, 1. Ishida, K.; Morokuma, K.; Komornicki, A. *J. Chem. Phys.* **1977**, *66*, 2153.

(19) A movie file has been deposited with the Supporting Information.

(20) A detailed analysis of the changes in bond lengths and angles in this process is included in the Supporting Information.

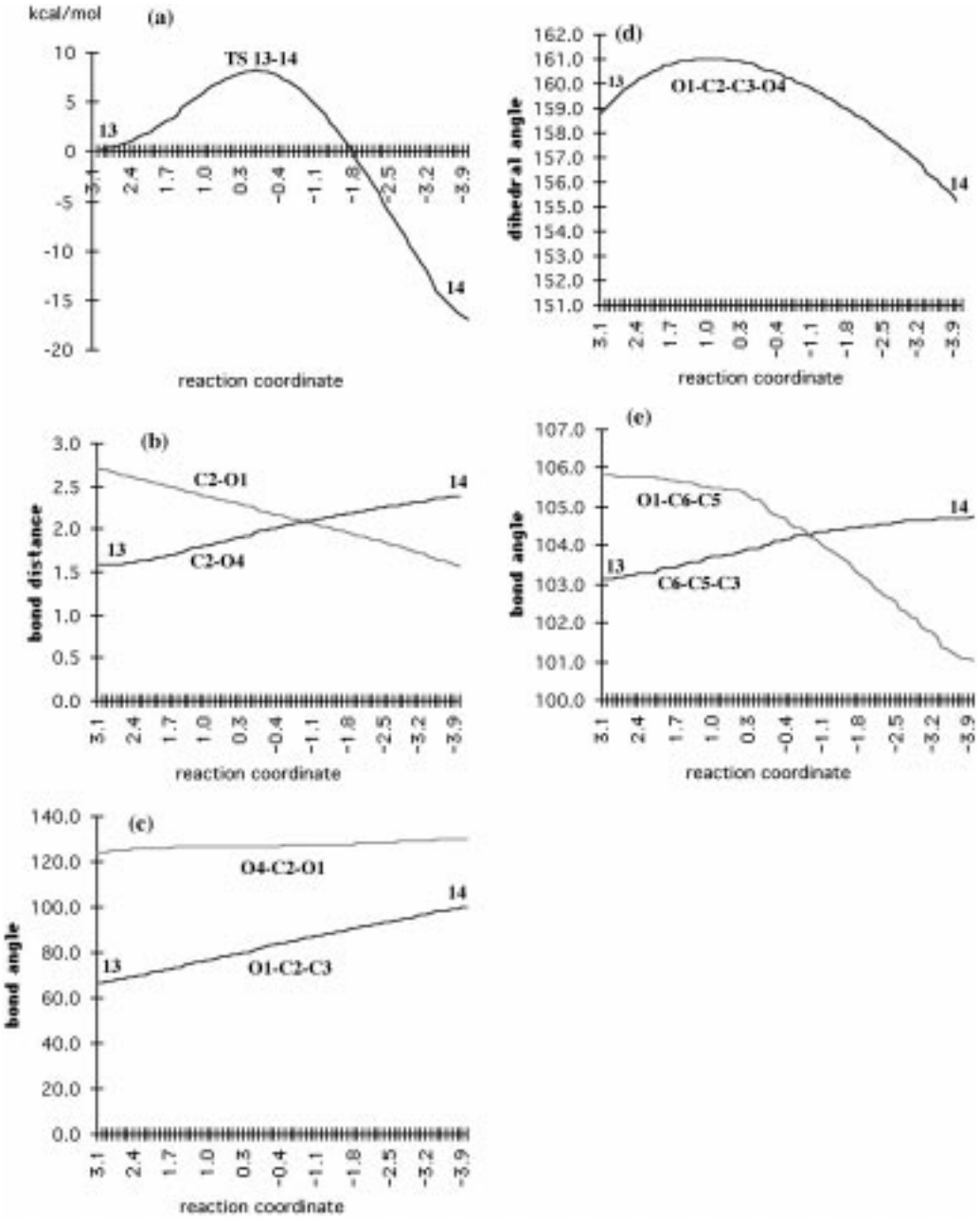

Figure 8. Intrinsic reaction coordinate (IRC) analysis for rearrangement of **13** to **14**. The abscissa in each figure is the reaction coordinate s in au·amu$^{1/2}$, with $s = 0$ corresponding to the transition state. Distances are in Å and angles are in deg. (a) Energy. (b) C2−oxygen distances. (c) Bond angles and (d) torsional angle, representing the nucleophile attack. (e) Internal bond angles.

the intramolecular hydroxyl to participate in concert with cleavage of the protonated epoxide would reduce the requirement for hyperconjugative stabilization of the developing charge at the carbon center where the reaction occurs.

The experimental results for this reaction show no evidence for products that would arise from the four-membered transition structure, and the yield of **11** is high (86%). The relative activation energy difference of four- to five-membered ring formation is calculated to be outside the energy window where such a process would be experimentally observed.

The minor product of the reaction of **9** with boron trifluoride was **12**, a product that cannot be formed by a route involving inversion of configuration. A search for a transition structure for retention of configuration from **16** to **14** was unsuccessful, and it is not likely to exist. Only one transition structure with retention of configuration leading to **14** from the trans epoxide was found at the HF/6-31G*, B3LYP/6-31G*, and MP2/6-31G* levels. This transition structure **TS 22**−**14** results from reaction of the protonated epoxide diastereomer **22**, shown in Figure 10.

The energy of this transition structure is higher by 10.8 and 8.1 kcal/mol at MP2/6-31G* and B3LYP/6-31G* levels, respectively, than that of **TS 16**−**18**, resulting from inversion of configuration from the protonated epoxide diastereomer **16**. This large energy difference suggests that **14** is formed not by a retention mechanism but most likely via the intermediacy of fluorohydrin. For the reaction catalyzed with BF_3·Et_2O, **12** is the minor reaction product (8%).

For the retention transition structure **TS 22**−**14**, hyperconjugation is observed between a methyl hydrogen

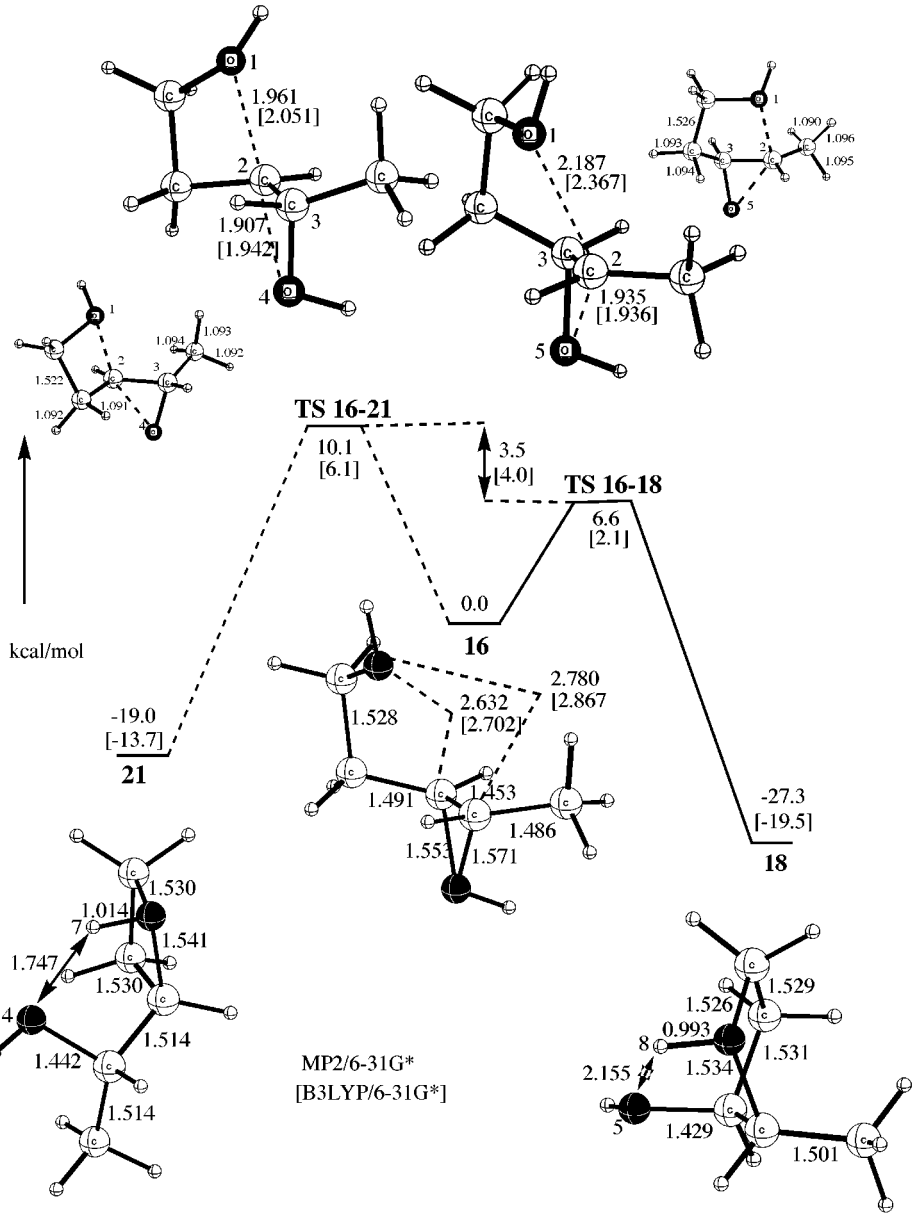

Figure 9. Potential energy profile for rearrangement of protonated *trans*-3,4-epoxypentan-1-ol (**16**) to **18** and **21**, both with retention of configuration. Geometries (in Å and deg) at the MP2(full)/6-31G* level. Two perspectives of each transition structure are shown. The relative energies in two levels (MP2(full)/6-31G*, B3LYP/6-31G* in brackets) are in kcal/mol and include zero-point corrections.

and the carbocation, indicative of a more pronounced development of charge at the reacting center than for **TS 16−18**.

The Intrinsic Reaction Coordinate (IRC) Analysis of the Rearrangement: 16 → TS 16−18 → 18. An intrinsic reaction coordinate calculation (IRC) was performed at the MP2/6-31G* level for the more favored reaction pathway **16 → TS 16−18 → 18** involving the five-membered transition structure.[19] In this pathway, the intramolecular hydroxyl preferentially approaches the reacting center from the reverse face at the site of epoxide cleavage to give the product of inversion of configuration, as seen in Figure 9.

The IRC,[21] shown in Figure 11, indicates that the transition structure **TS 16−18** is reached from the diastereomeric protonated epoxide **16** with the epoxide proton syn to the methyl and leads to the low-energy diastereomer **18**, which exhibits intramolecular hydrogen bonding between the ether proton and the hydroxyl (2.155 Å) with the proton on the ether oxygen syn to the methyl.

The overall reaction profile in Figure 11, like that for **13** in Figure 8a, is consistent with intramolecular nucleophilic attack occurring from the reverse face at the site of epoxide cleavage in concert with epoxide cleavage resulting in the product of inversion of configuration. The exothermic nature of the process reflects the driving force of the reaction, namely the relief of epoxide ring strain.

Conclusion

The intramolecular inversion transition structures for the reaction of **13** and **16** at the B3LYP/6-31G* and MP2/

(21) A detailed analysis of the IRC is given in the Supporting Information.

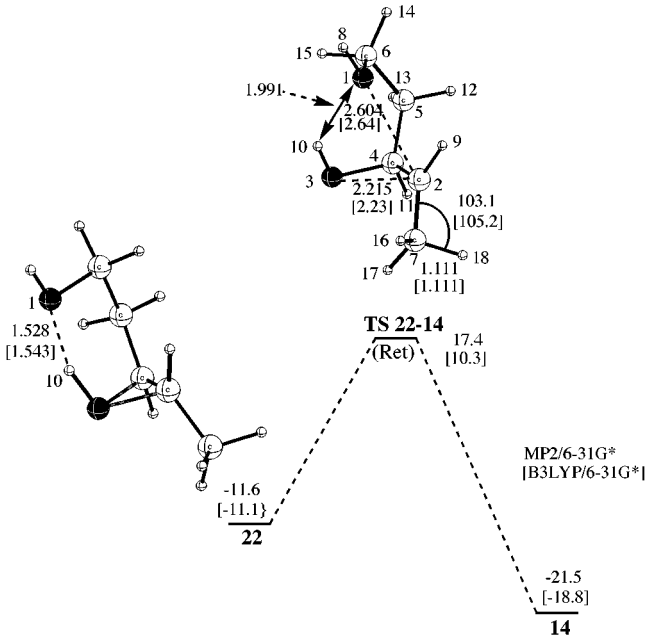

Figure 10. Potential energy profile for rearrangement of **22** to **14** with retention of configuration, compared with that of **16** to **18**. Geometries (in Å and deg) at the MP2(full)/6-31G* level. The energies relative to **16** in two levels (MP2(full)/6-31G*, B3LYP/6-31G* in brackets) are in kcal/mol and include zero-point corrections.

6-31G* levels of theory reveal a preference for five-membered ring formation. Intrinsic reaction coordinate calculations for the formation of **14** from **13** and **18** from **16** show that intramolecular attack with inversion occurs in concert with ring opening. The retention transition structures **TS 17**−**18** and **TS 22**−**14** are calculated to be too high in energy to afford credible pathways in the formation of **18** and **14**, respectively, and point to alternative pathways such as the intermediacy of fluorohydrin. The intrinsic reaction coordinates for inversion

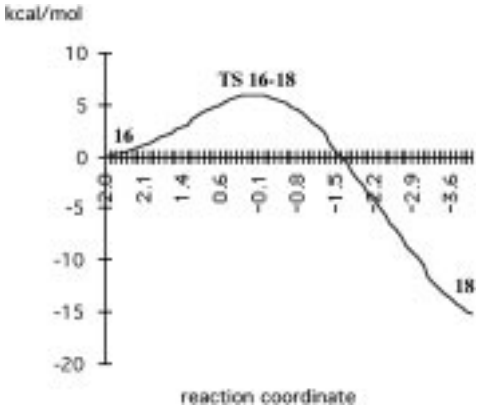

Figure 11. Intrinsic reaction coordinate (IRC) analysis for rearrangement of **16** to **18**. The abscissa is the reaction coordinate s in au·amu$^{1/2}$, with $s = 0$ corresponding to the transition state.

reaction of the nucleophile for the formation of **14** from **13** and **18** from **16** are far from optimum overlap and reflect the strained bicyclic nature of the transition structures.

Acknowledgment. One of us (J.M.C.) acknowledges a Emerson Visiting Fellowship at the Cherry L. Emerson Center for Scientific Computation, Emory University. We (J.M.C. and D.W.) acknowledge a NSF(US)-NZ Joint collaborative research award funded by NSF(US) and MOS(NZ) and grants from the New Zealand Lotteries Board.

Supporting Information Available: Archive material on all stationary points (21 pages) and an electronic file containing cis and trans hydroxy epoxide data that is available via the World Wide Web. This material is contained in libraries on microfiche, immediately follows this article in the microfilm version of the journal, and can be ordered from the ACS; see any current masthead page for ordering information.

JO972071V